Compressible and incompressible stripes in a narrow electron channel

D. Schmerek,* S. Manus, A. O. Govorov,[†] W. Hansen,* and J. P. Kotthaus

Sektion Physik der Ludwig-Maximilians-Universität Geschwister-Scholl-Platz 1, 80539 München, Germany

M. Holland

Department of Electronics and Electrical Engineering, University of Glasgow, Glasgow G128QQ, United Kingdom

(Received 13 June 1996; revised manuscript received 2 August 1996)

The capacitance of a single-electron wire at high quantizing magnetic fields is studied. We demonstrate that the capacitance spectroscopy allows us to study the formation of compressible and incompressible stripes directly. The electron wire is field induced in a metal insulator semiconductor heterostructure beneath a center gate. The electrostatic potential defining the wire edge is controlled by a tuning-fork-shaped electrode that encloses the center gate. It is found that the capacitance spectra are very sensitive to the wire edge potential and show a clear asymmetry of the capacitance minimum at filling factor $\nu = 2$. The experimental results are well described by a simple model considering the contribution of compressible and incompressible stripes in the electron channel, to the capacitance signal. The capacitance minima are thus determined in our experiments by the geometry of the compressible and incompressible stripes in the channel and not by the defect-induced density of states. [S0163-1829(96)02143-1]

The concept of edge states is presently favorably used to explain transport properties of two-dimensional electron systems (2DES's) in very high magnetic fields.[1,2] From the electrostatics at the electron channel edge in a split gate device, it is found that the filling-factor-dependent screening property of the electron system leads to the formation of alternating stripes of compressible and incompressible liquid phases aligned along the sample edge.[3] Transport as well as capacitance studies[4,5] have been performed in order to substantiate the model experimentally. Capacitance measurements are sensitive to the compressible phases in the channel only, and thus they can give quite direct information about the geometry of the compressible stripes at the sample edge. Recent capacitance measurements on two-dimensional electron channels with gates that overlap the channel edges have been interpreted on these terms.[4] It has been found that at integer filling factors in the quantized Hall effect regime, the capacitance is proportional to the edge of the sample, indicating that the edge alone contributes to the capacitance signal. In the experiment[4] it has been essential, that charge injection into 2DES beneath the gate takes place by lateral transport within the 2DES alone.[6] The differential capacitance is thus related to edge channels only at integer filling factors where the diagonal conductivity is sufficiently small. In contrast, in previous experiments[7] the 2DES was charged from a back electrode with very low mobility so that even at integer filling factors in the quantum Hall regime the localized states in the center of the sample can be charged.[7] In both cases[4,7] the shape of the capacitance minima is symmetrical, and determined by the defect-induced density of states (DOS) in the whole channel.

In the work presented here, similar devices to those used in Ref. 7 are employed for capacitance measurements, so that lateral transport in the 2D channel does not play an essential role. Furthermore, the probed channels are relatively narrow, so that the contributions of the central region and the channel edge to the capacitance signal are of comparable size. There-fore the channel edges dominate the experimental results, whereas potential fluctuations arising from imperfections play a minor role. This allows us to analyze quantitatively the filling factor dependency of the differential capacitance with a model that is based on the geometry of the edge states instead of the defect-induced DOS. Furthermore, in our experiments we can control the steepness of the channel edge potential with a tuning-fork-shaped gate. This allows us to test the sensitivity of the capacitance spectra on the channel edge potential.

The design of our samples is illustrated in Fig. 1. The essential layers of our epitaxially grown heterostrucures consist of a highly doped back electrode, a GaAs spacer layer, and a front barrier composed of a AlAs/GaAs short-period superlattice. They are identical to the layers of a previous publication,[8] where the effect of the one-dimensional subband quantization on the capacitance signal in extremely narrow quantum wires was investigated. On the crystal surface, finely structured metal electrodes are defined by electron-beam lithography and thermal evaporation. A center gate is formed by a 300-nm-wide and 100-μm-long metal stripe. This gate is enclosed by two gate stripes each separated by 150 nm from the edge of the center gate. The electron channel is field induced beneath the central gate at the interface between the barrier and the GaAs spacer layer if the central gate is biased with respect to a metallic back electrode at voltages V_1 that are larger than a distinct threshold voltage V_{th}. The form of the electrostatic potential at the channel edges is controlled by the potential V_2 applied at the side gates with respect to the back electrode.

Since the sample capacitance is small, the measurements are performed with a capacitance bridge arrangement where the sample and reference capacitance are prepared on the same crystal. This technique is similar to the one applied previously by Ashoori *et al.*[9] to record the single-electron charging of a quantum dot. The modulation of the balance point is detected with a phase-sensitive amplifier via an im-
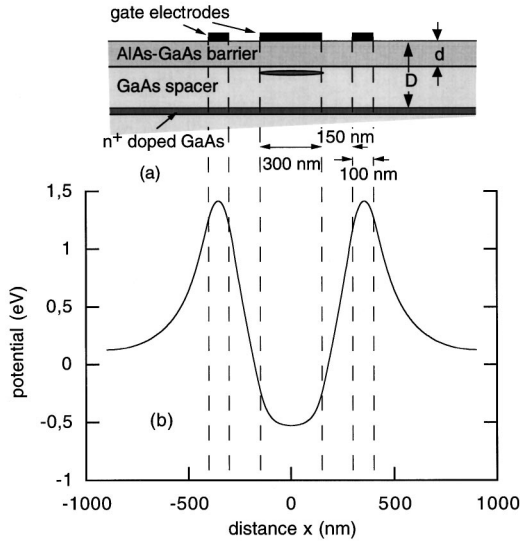
FIG. 1. (a) Cross section of a sample with relevant parameters for the widths and separation of the gate stripes, the thicknesses of the barrier and the GaAs spacer layer that separate the interface at which the electron channel resides from the gate and the back electrode, respectively: $d=42$ nm and $D=142$ nm. (b) Bare potential created by the gate electrodes biased at $V_1=0.8$ V and $V_2=-2.4$ V in the plane of the electron channel as calculated by a numerical integration of the Poisson equation. The lateral scale is chosen to match with the cross section in (a).

FIG. 2. The full line presents the differential capacitance of a sample recorded as function of the gate voltage V_1 at $\Delta V=3.2$ V and a magnetic field of $B=6.5$ T. The dashed line is calculated according to a model described in the text.

pedance transformer which is set up very closely to the sample. The conversion ratio from voltage signal at the amplifier input to the capacitance change in the sample is calculated from the amplification of the impedance transformer and the parasitic impedance between the balance point and ground. Since the latter is not well known, the absolute value of the conversion ratio is cross-checked with the capacitance calculated for an arrangement of metallic electrodes with a geometry such as that in the experimental device. For the calculation the electron channel is assumed to form a purely metallic electrode with 300-nm width, a value that we expect to be close to the real one at high electron density. From the above considerations we expect the conversion ratio not to deviate by more than 25% from the exact value.

In Fig. 2 we present the differential capacitance of the electron channel as a function of the center gate voltage V_1 at temperature 4 K. The measurement was performed at an excitation amplitude of 2 mV, a frequency of 100 kHz, and at a magnetic field of 6.5 T applied perpendicular to the channel. The potential difference between the center gate and the side gates $\Delta V=V_1-V_2$ was kept constant at $\Delta V=3.2$ V during the measurement so that the shape of the bare confining potential induced by the electrodes is approximately kept constant. At gate voltage $V_1\geq V_{th}=0.82$ V the electron channel is created as reflected by an increasing capacitance. We note that the increase is relatively smooth as compared to reference measurements in samples with wide gates. A small capacitance minimum appears at $V_1=0.95$ V, and a much more pronounced one is observed around $V_1=1.1$ V. In contrast to samples with wide gates, a characteristic property of the capacitance minima observed in our narrow stripe samples is a clear asymmetry: a steep decrease of the capaci-
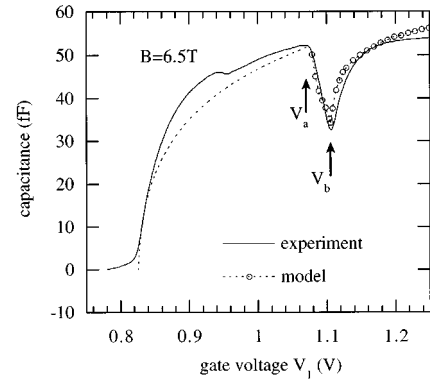
tance signal is followed by a smooth increase.

In the following we discuss the strong minimum at $V_1=1.1$ V in a model[10] that attributes this minimum to the creation of an incompressible stripe at filling factor $\nu=2$ in the center of the channel. The small minimum at $V_1=0.95$ V is associated with the spin gap at filling factor $\nu=1$, since the spin gap $g^*\mu_B B$ is much smaller than the Landau gap $\hbar\omega_c$ in GaAs.

According to recently developed models[3] in strong magnetic fields, the electron channel decomposes into stripes of compressible and incompressible liquid with local electron densities between or precisely at integer filling factors, respectively. In the model by Govorov[10] the capacitance is simply given by $C=\epsilon\epsilon_0 S_{comp}/d$ where d is the distance of the electron channel to the front electrodes. Thus the magnetocapacitance signal is proportional to the surface area S_{comp} of the compressible phase in the channel. This approach seems plausible as long as the widths of the compressible and incompressible stripes are large in comparison to d. Although this assumption may not be perfectly justified in our experimental system we would like to adopt it, because of the straightforward analysis that becomes possible with it. In addition, for the sake of simplicity we would like to assume, like in Ref. 10, that the spin degeneracy is not lifted in our experiments.

The gate voltage range covered in our experiment may be divided into three different regions: $V_{th}<V_1<V_a$ where the compressible stripe of the first Landau level is filled; $V_a<V_1<V_b$, where the first incompressible stripe evolves, and $V_b<V_1<V_c$, where the compressible stripe of the second Landau level arises. As depicted in Fig. 2, the voltages V_a and V_b coincide with the maximum and minimum in the capacitance trace, respectively. The voltage V_c is beyond the experimental values shown in our figures.

In the view of our simple model, the gradual increase of the capacitance signal between the threshold voltage V_{th} and V_a directly reflects the evolution of the width of the compressible stripe. The width rises with the center gate voltage as long as the density is smaller than a density n_L that corresponds to a completely filled spin degenerate Landau level. The local electron density is highest in the center of the channel, and gradually decreases to the edge. When the local

electron density in the channel center reaches n_L, an incompressible stripe arises that divides the compressible region into two stripes. At this point the capacitance reaches a local maximum, since — within reasonable assumptions for the confinement potential — the area of the compressible stripes decreases when the incompressible stripe rapidly evolves.

To compare the experimental data with our model, quantitatively we have to know the form of the so-called bare confinement potential in the plane of the electron channel. In Ref. 10, explicit results for the model were derived assuming a parabolic confinement potential. However, with a parabolic potential the experimental traces are poorly described. We determine the bare potential numerically by solving the Poisson equation with boundary conditions dictated by the potentials of the metallic electrodes at the threshold voltage, and assuming no charges at the semiconductor vacuum interface between the gate electrodes. The confinement potential for $\Delta V = 3.2$ V thus evaluated is shown in the lower part of Fig. 1. In Ref. 10 a simple recipe is derived to generalize the model for arbitrary confinement potentials: If the confinement is described by a function $\phi_0(x,d^*) = \phi_0(0,d^*) - f(x)$, the width of the electron channel W and thus the capacitance are essentially proportional to the inverse $f^*(x)$ of the function $f(x): W = 2f^*[\phi_0(0,d^*)]$. In Ref. 10 the value $\phi_0(0,d^*)$ was assumed to be equal to the applied gate voltage (valid for $D \gg d^*$). For our device a geometrical lever arm $\lambda = D/(D - d^*)$ has to be introduced that takes into account the finite distance d^* between the gate and the electron channel: $\phi_0(0,d^*) = (V_1 - V_{th})/\lambda$. Here $(x=0, z=0)$ points to the middle of the center gate, and d^* is the distance between the center of the electron charge distribution in the channel and the gate. We derived a value of $d^* = 56$ nm from the gate voltage separation of the magnetocapacitance minima in reference samples with wide gates.

The capacitance calculated within our model from this confinement potential is depicted in Fig. 2 together with the experimental data. The calculated capacitance increases smoothly above the threshold voltage, similar to the experimental curve and describes the data much better than any parabolic confinement potential. We would like to point out that, except for V_{th}, our modeled capacitance contains no free parameter. In view of the precision with which we can determine the absolute capacitance value, we thus find very good quantitative agreement with the experiment.

The capacitance maximum is expected to occur when the local electron density reaches $n_L = 2eB/\hbar$ in the center of the channel. The corresponding gate voltage V_a is determined by $V_a - V_{th} = en_L d^*/\epsilon\epsilon_0$, and is thus independent of the lever arm or the form of the confinement potential. The experimental value coincides well with the calculated one. At a higher gate voltage $V_a < V_1 < V_b$, the first incompressible stripe arises. Since it is expected that the original model[10] is only a first approximation if the width of the incompressible stripe $2a_1$ is of order d^*, we simulated this situation by numerical solution of the Poisson equation for variable gaps between the compressible stripes which are represented by thin metallic stripes. As expected, we find in our calculations that the value of the potential minimum between the metallic stripes is much lower than $(V_1 - V_a)/\lambda$, especially for small a_1. To improve the model we introduce a lever arm $\lambda(a_1)$ that is found by our simulation calculation. Since the width
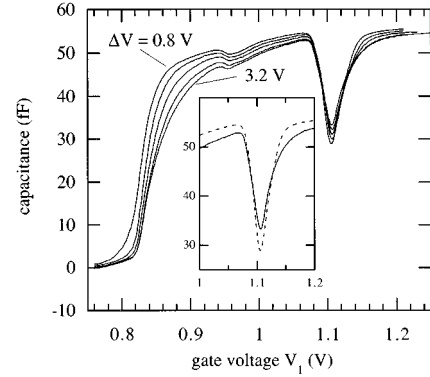

FIG. 3. Capacitance traces of the same device as in Fig. 2 recorded at different voltage differences ΔV between center gate and side gates. The bottom trace is recorded at $\Delta V = 3.2$ V and the difference is decreased in steps of 0.6 V. The inset depicts the behavior at filling factor $\nu = 2$ for $\Delta V = 3.2$ V (full line) and 0.8 V (dashed line), respectively.

$a_1 = f^*[(V_1 - V_a)/\lambda(a_1)]$ depends on the lever arm $\lambda(a_1)$, the values of $\lambda(a_1)$ and a_1 have to be determined self-consistently for each gate voltage. We use an iteration that starts with $\lambda^0 = D/(D - d^*)$. With the resulting value for the gap width $a_1^0 = f^*[(V_1 - V_a)/\lambda^0]$, we solve Poisson's equation to obtain a value λ^1 for the next iteration loop. This procedure converges very fast. The data points denoted by open circles in Fig. 2 were calculated in this way. The dashed line represents a guide to the eye at $V_1 > V_a$. The value of V_b is given by $(V_b - V_a)/\lambda(a_1) = \hbar\omega_c$, with $a_1 = f^*(\hbar\omega_c) = 47$ nm and $\lambda(a_1) = 3$. We thus find $V_b - V_a = 32$ mV, in excellent agreement with the experiment.

At $V_1 > V_b$ the capacitance rises again as a result of the formation of the compressible stripe in the second Landau level. Corresponding to our model, the width of this stripe is given by $f^*[(V_1 - V_b)/\lambda(a_1)]$. We would like to point out that our simple model nicely explains the clear asymmetry found in our experimental trace. This asymmetry thus is a characteristic property of a device where the magnetocapacitance at integer filling factors is no longer dominated by impurity-related potential fluctuations in the bulk of the channel, but by the potential and geometry of compressible phases in the channel.

In Fig. 3 we depict capacitance traces of our device recorded at various potential differences ΔV between the center gate and the side gates. The data clearly show a steeper onset of the capacitance with decreasing bias at the side gates. This is expected, since at smaller ΔV the bottom of the bare potential becomes flatter, and correspondingly the function f^* rises more rapidly with V_1. This is also the reason for the deeper minima at the smaller ΔV, which can be clearly seen in the inset of Fig. 3.

In conclusion, we investigated a narrow 2DES channel with magnetocapacitance at magnetic fields that suffice for the development of compressible and incompressible stripes. In our devices the channel width is comparable to the width of the compressible stripes. Usually, the shape of the capacitance minima is symmetric in devices where the capacitance reflects the impurity-related DOS between the Landau levels.

In our devices the minima have a clear asymmetry, and it is demonstrated that the shape of the capacitance spectra is very sensitive on the channel edge potential. We interpret our data with a model that directly associates the behavior of the capacitance as a function of the gate voltage with the surface area of the compressible and incompressible states. Thus the asymmetry originates from the electrochemical nature of the magnetocapacitance and the electron-electron interaction, which results in the formation of alternating compressible and incompressible liquids in a 2D magnetoplasma.

---

[*] Present and permanent address: Institut für Angewandte Physik, Universität Hamburg, Jungiusstr. 11, 20355 Hamburg, Germany.

[†] Permanent address: Institute of Semiconductor Physics, 630090, Novosibirsk-90, Russia.

[1] B. I. Halperin, Phys. Rev. B **25**, 2185 (1982).

[2] M. Büttiker, in *Nanostructured Systems*, edited by R.K. Williardson, A.C. Beer, and E. R. Weber, Semiconductors and Semimetals Vol. 35 (Academic, San Diego, 1992), p. 191.

[3] D. B. Chklovskii, B. I. Shklovskii, and L. I. Glazman, Phys. Rev. B **46**, 4026 (1992); D. B. Chklovskii, K.A. Matveev, and B. I. Shklovskii, *ibid.* **47**, 12 605 (1993).

[4] S. Takaoka, K. Oto, H. Kurimoto, K. Murase, K. Gamo, and S. Nishi, Phys. Rev. Lett. B **72**, 3080 (1994).

[5] W. Chen, T. P. Smith III, M. Bttiker, and M. Shayegan, Phys. Rev. Lett. B **73**, 146 (1994).

[6] M. Büttiker, J. Phys. Condens. Matter **5**, 9361 (1993).

[7] T. P. Smith III, W. I. Wang, and P. J. Stiles, Phys. Rev. B **34**, 2995 (1986).

[8] H. Drexler, W. Hansen, S. Manus, J. P. Kotthaus, M. Holland, and S. P. Beaumont, Phys. Rev. B **49**, 14 074 (1994).

[9] R. C. Ashoori, H. L. Strmer, J. S. Weiner, L. N. Pfeiffer, K. W. Baldwin, and K. W. West, Phys. Rev. Lett. **71**, 613 (1993).

[10] A.O. Govorov, Phys. Rev. B **51**, 14 498 (1995).